J Mol Model (2008) 14:1159–1172
DOI 10.1007/s00894-008-0358-0

ORIGINAL PAPER

Theoretical study of the kinetics and mechanism of the decomposition of trifluoromethanol, trichloromethanol, and tribromomethanol in the gas phase

Katarzyna Brudnik · Dorota Wójcik-Pastuszka · Jerzy T. Jodkowski · Jerzy Leszczynski

Received: 28 January 2008 / Accepted: 11 September 2008 / Published online: 15 October 2008

Abstract Ab initio calculations at the G2 level were used in a theoretical analysis of the kinetics of unimolecular and water-accelerated decomposition of the halogenated alcohols CX_3OH (X = F, Cl, and Br) into CX_2O and HX. The calculations show that reactions of the unimolecular decomposition of CX_3OH are of no importance under atmospheric conditions. A considerably lower energy pathway for the decomposition of CX_3OH is accessible by homogenous reactions between CX_3OH and water. It is shown that $CX_3OH + H_2O$ reactions proceed via the formation of intermediate complexes. The mechanism of the reactions appears to be complex and consists of three consecutive elementary processes. The calculated values of the second-order rate constants are of 2.5×10^{-21}, 2.1×10^{-19}, and 1.2×10^{-17} $cm^3molecule^{-1}s^{-1}$ at 300 K for $CF_3OH + H_2O$, $CCl_3OH + H_2O$, and $CBr_3OH + H_2O$, respectively. The theoretically derived atmospheric lifetimes of the CX_3OH molecules indicate that the water-mediated decomposition reactions $CX_3OH + H_2O$ may be the most efficient process of CF_3OH, CCl_3OH, and CBr_3OH loss in the atmosphere.

Keywords Kinetics · Tribromomethanol · Trichloromethanol · Trifluoromethanol

K. Brudnik · D. Wójcik-Pastuszka · J. T. Jodkowski (✉)
Department of Physical Chemistry, Wroclaw Medical University,
pl. Nankiera 1,
50–140 Wroclaw, Poland
e-mail: jurek@kchfiz.am.wroc.pl

J. Leszczynski
Department of Chemistry, Jackson State University,
1400 J.R. Lynch Street,
Jackson, MS 39217, USA

Introduction

The halogenated alkyl radicals are mainly produced during the photofragmentation of halocarbons and take part in many degradation processes proceeding in the atmosphere and in various combustion systems [1]. The only significant atmospheric fate of alkyl radicals is the addition reaction with molecular oxygen. In the oxygen-rich atmosphere, the halogenated methyl radicals CF_3, CCl_3, and CBr_3 are converted into the methylperoxy structures CX_3O_2 (X = F, Cl, and Br), which then react with nitric oxide generating trifluoro-, trichloro-, and tribromomethoxy CX_3O radicals [2, 3]. The subsequent fate of the CX_3O radicals is considerably less known. Kinetic studies suggest that the primary loss of CX_3O radicals in the lower atmosphere is related to reactions with nitrogen oxides, NO and NO_2. Alternatively, reactions between CX_3O and H_2O or hydrocarbons (RH) lead to the formation of the respective perhalogenated alcohols:

$$CX_3O + (H_2O, RH) \rightarrow CX_3OH + (OH, R) \quad (1)$$

which are able to act as temporary halogen reservoir species. The subsequent removal of CX_3OH is thus important in understanding the possible processes of CX_3O radical loss. Therefore the decomposition of CX_3OH has become the subject of several experimental and theoretical investigations [4–23].

The decomposition of CF_3OH has been the most frequently studied [4–18]. Kinetic investigations indicate that the reactions of hydrogen abstraction from CF_3OH are related to a high activation energy and proceed too slowly to be of importance in atmospheric chemistry. The photolysis of CF_3OH to regenerate CF_3O radicals is also inefficient. There is therefore no known mechanism by which CF_3OH can be readily converted back into CF_3O

radicals in the stratosphere. The unimolecular decomposition of CF_3OH with the elimination of hydrogen fluoride:

$$CF_3OH \rightarrow COF_2 + HF \quad (2)$$

is thought to be the main atmospheric fate of CF_3OH. Reaction (2) appears to be an endothermic process with a very high activation energy. Values for the energy barrier of over 40 kcal mol^{-1} have been calculated at various levels of theory [4, 8, 13]. This height of the energy barrier for the homogeneous decomposition of CF_3OH implies a negligible reaction rate under ambient atmospheric conditions. However, kinetic experiments show that CF_3OH decomposes readily to yield CF_2O, strongly suggesting that the reaction is most likely accelerated by the interaction of CF_3OH with other molecules on the surface of the reaction chamber [24]. There is evidence that water can introduce many unusual features into the kinetics and energetics of chemical reaction systems [25–27]. The introduction of water vapor into the reaction chamber leads to acceleration of the presumably heterogeneous decomposition of CF_3OH [24]. This is why the incorporation of CF_3OH into water droplets or its decomposition on aerosols are thought to dominate the loss processes of atmospheric CF_3OH. Results of ab initio calculations show the existence of a lower energy pathway on the potential energy surface available in the reaction system $CF_3OH + H_2O$ [13]. The decrease in the energy barrier causes an increase in the reaction rate, which is consistent with the experimentally observed catalytic influence of water on the decomposition of CF_3OH.

The analogous reaction of the decomposition of trichloromethanol CCl_3OH to phosgene $COCl_2$ and HCl:

$$CCl_3OH \rightarrow COCl_2 + HCl \quad (3)$$

was studied theoretically and in several smog-chamber experiments [19–23]. The kinetic behavior of CCl_3OH was found to be similar to that of CF_3OH. The measured rate of CCl_3OH decay grows with increasing contact of the reactant molecules with the surface of the reactor walls, suggesting a heterogeneous mechanism of CCl_3OH decomposition. An upper limit of the overall rate constant k_3 of 1.05×10^{-2} s^{-1} was estimated [20]. On the other hand, the energy barrier derived from ab initio calculations at the CCSD(T)/cc-pVTZ level [20] is high, i.e., 31 kcal mol^{-1}. This corresponds to a value of 2×10^{-10} s^{-1} for the first-order rate constant k_3 for the homogeneous decomposition of CCl_3OH calculated using a conventional transition state theory approach. It is far less than the upper limit derived from experiments.

To the best of our knowledge there is no experimental and theoretical information on the kinetics of the unimolecular decomposition of CBr_3OH:

$$CBr_3OH \rightarrow COBr_2 + HBr \quad (4)$$

However, the similarity of the structural parameters and molecular properties of CBr_3OH to CCl_3OH and CF_3OH suggests that the mechanism of CBr_3OH decomposition is likely analogous to reactions (2) and (3).

The primary aim of the present theoretical investigations is to achieve a better understanding of the kinetics and mechanism of the atmospheric decomposition of the halogenated methyl alcohols CX_3OH (X = F, Cl, and Br). The experimental findings indicate that the presence of water molecules plays an important role in promoting CF_3OH and CCl_3OH decomposition [13, 19]. The simplest model enabling us to explain and describe the role of water molecules in the mechanism of CX_3OH decomposition is based on analysis of the calculated potential energy surface of the reaction system consisting of CX_3OH and a single H_2O molecule. This analysis involves the ab initio search for the bound complexes, transition states, and their structural and molecular characteristics. The stationary points of the potential energy surface of the molecular system $CX_3OH + H_2O$ correspond to the molecular structures taking part in the reaction:

$$CX_3OH + H_2O \rightarrow COX_2 + HX + H_2O \quad (5)$$

Results of the high-level ab initio calculations should provide useful information to gain insight into the reaction mechanism and to evaluate the rate constants using the computational methods of the reaction rate theory.

Computational details

All quantum mechanical ab intio calculations were carried using the Gaussian 03 program package [28]. Electron correlation was estimated by Møller-Plesset perturbation theory at the second (MP2) and up to the fourth order including all single, double, triple, and quadruple excitations (MP4SDTQ). The frozen core approximation was kept throughout. Total electronic energies for the open-shell systems were calculated with a projection method and are denoted by PMPn. The geometries of all stationary point structures of the potential energy surface were fully optimized at both the SCF and MP2 levels with the 6–31G(d) basis set. Relative total energies were examined using G2 methodology [29]. This approach requires some additional calculations at the MP4/6–311G(d,p), MP4/6–311+G(d,p), MP4/6–311G(2df,p), MP2/6–311 + G(3df,2p), and QCISD(T)/6–311G(d,p) levels using the MP2/6–31G (d) optimized geometry as a reference to obtain improved energy values.

The rate constants of the reactions studied were analyzed in terms of conventional transition-state theory (TST) [30,

31]. The thermochemical formulation of TST leads to the rate constant, k_{TST}, given by

$$k_{TST} = \sigma \frac{k_B T}{h} \exp\left(\frac{\Delta S^{\neq}}{R}\right) \exp\left(-\frac{\Delta H^{\neq}}{RT}\right), \quad (6)$$

where σ denotes a symmetry factor related to reaction path degeneracy, k_B and h are the Boltzmann and Planck constants, respectively, $\Delta S^{\neq}$ is the activation entropy, and $\Delta H^{\neq}$ the activation enthalpy for the reaction under investigation. The vibrational and rotational contributions to the thermodynamic functions were derived by the classical harmonic-oscillator rigid-rotor approximation (no free or internal rotation was considered).

Results and discussion

It is well known that the G2 method [29] well reproduces the structural parameters and molecular properties of a wide group of organic compounds. The halogenated alcohols have become the subject of theoretical investigations at several levels of theory because of their possible role in the destruction of atmospheric ozone. Results of calculations show a distinct advantage of the G2 approach, which better reproduces the molecular properties of this class of compounds. The reliable values of the thermochemical properties and vibrational frequencies obtained by G2 methodology for perhalogenated methanols [15–17, 23, 32–34] favor the use of this level of theory for a description of the structural parameters of the investigated molecular systems. The geometry of the molecular structures taking part in the decomposition of the halogenated methanol molecules was optimized at both the SCF/6–31G(d) and MP2/6–31G(d) levels (with the exception of the H_2O and HX molecules, whose molecular parameters were taken from refs. [35–37]). The molecular arrangements and definitions of the structural parameters used in the geometry optimization are given in Fig. 1. The postulated catalytic role of the water molecule in the CX_3OH decomposition reaction must involve a change in the reaction mechanism related to the formation of loosely bound intermediate complexes of the reactants/products. Therefore, at each level of theory the potential energy surface was independently explored for the possible existence of transition states and intermediate complexes.

Thermal decomposition of CF_3OH

The numerical values of the optimized structural parameters of the species appearing in the decomposition of CF_3OH to CF_2O and HF are listed in Table 1. In the table are also the vibrational frequencies obtained in SCF/6–31G(d) calculations and scaled by 0.8929 as well as the G2-total energies at 0 K (ZPE included). A staggered conformation of C_s symmetry was predicted as the most stable molecular structure of CF_3OH. Except for the C–F bond lengths, the geometrical parameters of CF_3OH are very similar to those of methanol. Trifluoromethanol is found to be a molecular structure with an unusually strong CF_3O–H bond. The bond dissociation energy of CF_3O–H is distinctly greater than that of CH_3OH and comparable to or even slightly greater than that of HO–H in water. This anomalously large CF_3O–

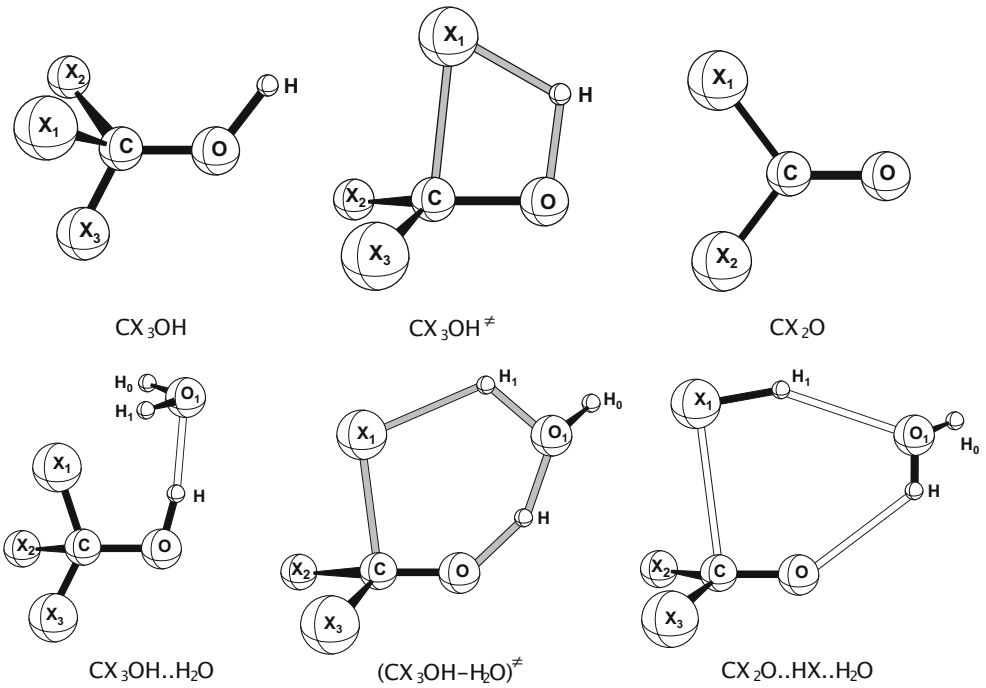

Fig. 1 Definition of the geometrical parameters of the molecular structures taking part in the mechanism of the reactions under investigation

Table 1 Molecular properties of the structures taking part in the reaction mechanism of the thermal decomposition of trifluoromethanol [a)]

	CF_3OH	TS1F	MC1F	TS2F	MC2F	CF_2O
CO	1.3511	1.2628	1.3325	1.2410	1.1936	1.1871
OH	0.9741	1.2545	0.9932	1.4803	2.0868	
CF_1	1.3520	1.7186	1.3648	1.6578	2.4753	1.3277
CF_2	1.3520	1.3168	1.3333	1.3405	1.3189	1.3277
CF_3	1.3317	1.3168	1.3648	1.3450	1.3174	
O_1H			1.7825	1.0579	0.9753	
O_1H_1			0.9724	1.0996	1.6679	
O_1H_0			0.9724	0.9769	0.9710	
COH	108.1404	80.7211	106.4097	111.1405	120.6088	
F_1CO	112.1963	91.0308	112.6075	109.1354	97.2129	126.2625
F_2CO	112.1963	121.7898	110.0766	119.3965	125.5856	126.2625
F_3CO	108.3109	121.7898	112.6075	119.8655	125.5329	
OHO_1			158.3480	148.2313	136.9347	
HO_1H_1			103.7736	91.1389	97.7270	
HO_1H_0			103.7736	107.1437	104.7259	
F_1COH	59.8927	0.0000	59.2997	15.9633	−25.3349	
F_2COH	−59.8927	106.4701	−59.2997	127.9787	65.8308	
F_3COH	180.0000	−106.4701	180.0000	−95.6167	−119.7674	
O_1HOC			0.0000	−21.0941	38.9245	
H_1O_1HO			54.3761	10.1937	−17.1051	
H_0O_1HO			−54.3761	−99.5733	97.2886	
υ_1	235	1758 i [b)]	22	744 i [b)]	22	563
υ_2	428	260	44	43	88	610
υ_3	441	336	79	297	95	779
υ_4	583	537	187	340	109	977
υ_5	607	551	243	352	136	1306
υ_6	617	684	275	387	159	1952
υ_7	889	823	420	483	237	
υ_8	1123	916	438	519	266	
υ_9	1235	981	595	561	409	
υ_{10}	1324	1389	604	602	567	
υ_{11}	1414	1617	617	604	612	
υ_{12}	3653	1973	715	772	688	
υ_{13}			887	943	776	
υ_{14}			1164	371	843	
υ_{15}			1210	1350	989	
υ_{16}			1352	1463	1338	
υ_{17}			1448	1584	1631	
υ_{18}			1626	1666	1917	
υ_{19}			3466	2019	3540	
υ_{20}			3628	2809	3618	
υ_{21}			3728	3617	3716	
E_0(G2)	−413.03877	−412.97890	−489.39556	−489.35253	−489.39182	−312.69122

[a)] G2 molecular parameters: geometrical structure optimized at the MP2/6–31G(d) level, (bond lengths in Å, valence and dihedral angles in degrees), the SCF/6–31G(d) vibrational frequencies υ_i (cm^{-1}) scaled by 0.8929 and the total G2-energies in a.u. at 0 K (ZPE included).
[b)] the unscaled MP2/6–31G(d) vibrational frequencies (cm^{-1})

H bond strength is usually attributed to the negative hyperconjugation effect of the CF_3 group [38].

The transition state $CF_3OH^{\neq}$ (TS1F) for the decomposition $CF_3OH \rightarrow CF_2O + HF$ also has C_s symmetry. Rotation of the OH group around the C–O axis causes both the C–F_1 and O–H bonds to become parallel and located on the symmetry plane F_1COH. The reorientation of the bonds is accompanied by a change in the valence angles; the C–F_1 and O–H bonds consequently become almost perpendicular to the C–O bond. The bond lengths of 1.25 Å for O–H and 1.72 Å for C–F_1 are 30% longer than those in CF_3OH. In contrast, the C–O bond of $CF_3OH^{\neq}$ is only slightly shorter than that of CF_3OH, whereas the valence angles of TS1F, i.e., F_2CO, F_3CO, and F_2CF_3, are close in value to the corresponding angles in the planar product molecule CF_2O. The relative total energy of the transition state $CF_3OH^{\neq}$

with respect to the reactant molecule is calculated as 37.6 kcal mol^{-1} at 0 K. This energy can be identified with the activation energy for the thermal decomposition of CF_3OH.

The molecular complex $CF_3OH...H_2O$, denoted by MC1F, is the most stable structure in the $CF_3OH + H_2O$ reaction system. The geometrical parameters, especially bond lengths and bond angles, of this hydrogen-bonding complex are very close to those in the isolated reactants, CF_3OH and H_2O. Only the O–H bond is longer by 0.02 Å and the C–O bond shorter by 0.02 Å than the corresponding bonds in CF_3OH. The symmetry plane assigned by the F_1–C–O–H–O_1 atoms implies C_s symmetry of MC1F. In this hydrogen-bonding complex, the H–O_1 contact distance of 1.78 Å is almost twice as long as that of the O–H bond in water and alcohols. The thermal stability of MC1F toward CF_3OH estimated at the G2 level is 15.5 kcal mol^{-1} at 0 K.

The saddle point TS2F $(CF_3OH..H_2O)^{\neq}$ describes the decomposition of trifluoromethanol in the presence of water. A displacement of H_2O from its location at the MC1F complex in the direction of the abstracted fluorine atom of CF_3OH leads to the formation of a six-atom-ring structure: C...F_1...H_1...O_1...H...O. In this way the formed hydrogen bonds serve as a molecular bridge connecting the water molecule with the H and F_1 atoms of CF_3OH. In consequence, the presence of the water molecule promotes the removal of the fluorine and hydrogen atoms from the alcohol. The symmetry plane F_1COH disappears and the dihedral angle F_1–C–O–H reaches a value of 25°. The transition state TS2F is a looser molecular structure than TS1F and has a symmetry of C_1 point group due to the lack of symmetry elements. The molecular transformation of the reactants leading to the formation of TS2F needs considerably less energy compared with the formation of TS1F from CF_3OH.

The post-reaction adduct $CF_2O...HF...H_2O$, denoted by MC2F, is a molecular structure consisting of three subunits, CF_2O, HF, and H_2O, bonded in a molecular complex. The geometrical parameters of these subunits are very close to the corresponding ones in the isolated molecules. The contact distances C...F_1, H_1...O_1, and O...H calculated at the MP2/6–31(d) level are 2.48, 1.67, and 2.09 Å, respectively. The dissociation energy of MC2F to the final reaction products, obtained from G2-total energies, is estimated 11.7 kcal mol^{-1} at 0 K.

The profiles of the potential energy surface calculated for the decomposition of CF_3OH in the absence (left side of the figure) and presence (right side) of water are shown in Fig. 2. The thermal decomposition $CF_3OH \rightarrow CF_2O + HF$ is an almost thermoneutral process and the heat of reaction depends only weakly on temperature. The calculated reaction enthalpy of -1.5 kcal mol^{-1} at 0 K changes to 0.2 kcal mol^{-1} at room temperature, but at temperatures over 850 K the reaction again becomes an exothermic process. Reaction (2) is related to a very high energy barrier of 37.6 kcal mol^{-1}, which implies either small values of the rate constant or its strong dependence on temperature. In the presence of water, the first elementary step of the reaction mechanism is related to the formation of the molecular complex MC1F. The next step leads via TS2F directly to the other molecular complex, MC2F, which dissociates to the final reaction products. An analysis of the structural parameters, especially the H...F_1 distances, in the critical molecular structures allows us to explain the catalytic role of the water molecule in the decomposition of CF_3OH. The bond distance of 2.42 Å between the H...F_1 atoms being removed from the CF_3OH molecule becomes 1.19 Å, i.e., half as long, in TS1F but remains almost unchangeable, at 2.36 Å, in TS2F. In consequence, the formation of TS2F requires fewer changes in the structure of the reactants than the formation of TS1F. Hence the water molecule plays the role of a molecular vehicle which supports the transport and exchange of hydrogen atoms inside the C...F_1...H_1...O_1...H...O ring. This results in a decrease in the activation barrier. The energy barrier for the reaction $CF_3OH + H_2O \rightarrow CF_2O + HF + H_2O$ is lower by 26.1 kcal mol^{-1} than the threshold energy for the $CF_3OH \rightarrow CF_2O + HF$ reaction. The presence of water vapor therefore distinctly accelerates the decomposition of the CF_3OH molecule.

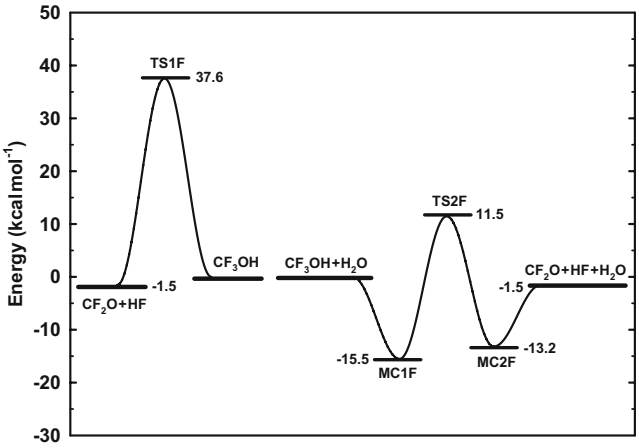

Fig. 2 Schematic energy profile for the decomposition of CF_3OH in the absence (left side) and presence (right side) of water. The energies are calculated at the G2 level including zero-point energy corrections

The energetics and the reaction path of the unimolecular decomposition of CF_3OH were previously studied at different levels of theory [4, 8, 13]. Results of calculations show that the reaction is endothermic at room temperature. Values available in literature of the reaction enthalpy corrected to room temperature vary, with 14.9 kcal mol^{-1}, 9.1 kcal mol^{-1}, and 5.0 kcal mol^{-1} calculated at the MP4/6-31G(d), QCISD(T)/6–311G(2df,2p), and MP4/TZ2P (triple-dzeta with polarization functions) levels [4, 8, 13], respectively.

The reaction enthalpies at 298 K calculated on the basis of the latest NASA [39] and IUPAC [40] recommended values for the enthalpy of the formation for CF_3OH, CF_2O, and HF lead to values of 2.8±2.5 [39] and 3.7±3.4 kcal mol^{-1} [40], respectively. The reaction enthalpy of 0.2 kcal/mol at 298 K calculated in this study at the G2 level corresponds to the lower limit of values obtained from thermodynamic tables. Our results indicate that the reaction is almost thermoneutral, but the sign of the calculated enthalpy depends on temperature. The reaction is weakly endothermic in the range of 250–850 K, but becomes exothermic at temperature below 250 K or above 850 K.

The presence of water vapor causes a distinct decrease in the reaction barrier for the decay of CF_3OH relative to the unimolecular pathway. Schneider et al. [13] have shown that the magnitude of the decrease in the height of energy barrier calculated at different levels of theory changes by between 25–29 kcal mol^{-1}, which is in line with the value of 26.1 kcal mol^{-1} derived from G2 calculations in this study. This indicates that the dimension of the basis set and the level of treatment of the electron correlation have a relatively small influence on the magnitude of the decrease in the energy barrier for the decomposition of CF_3OH in the presence of water molecules. More significant differences appear in the calculated values of the energy barrier at 0 K, which, calculated for the unimolecular decomposition of CF_3OH, are of 45.1, 43.9, 42.5, 42.1, and 37.6 kcal mol^{-1} at the QCISD(T)/6–311(2df,2p)//MP2/6–311G(2d,2p), MP2/SVP, MP2/TZ2P, MP4/TZ2P [4, 13], and G2 levels, respectively. The lowest energy barrier is that obtained at the G2 level; however, the height of the barrier still implies a negligibly slow reaction rate under atmospheric conditions.

The reported values of the calculated heights of the energy barrier for the water-mediated decomposition of CF_3OH retain an analogous ordering. The value of 11.5 kcal mol^{-1} obtained in this study at the G2 level is the lowest and is 3.5–5.5 kcal mol^{-1} lower than those obtained by Schneider et al. [13] at different levels of theory. The lower energy barrier predicted by the G2 method for the $CF_3OH + H_2O$ reaction has practical consequences because a decrease of the activation barrier by 3.5 kcal mol^{-1} leads to an increase in the reaction rate by a factor of 350 at room temperature. This may suggest some importance of the homogenous reaction $CF_3OH + H_2O$ for atmospheric chemistry.

Thermal decomposition of CCl_3OH

The optimized structural parameters, vibrational frequencies, and G2-total energies of the molecular structures taking part in the decomposition of CCl_3OH to CCl_2O and HCl are gathered in Table 2. The most stable structure of CCl_3OH appears to possess a staggered conformation with C_s molecular symmetry. The only significant difference in the geometrical parameters of CF_3OH and CCl_3OH is related to the C–F and C–Cl bond lengths. The other bond lengths and angular parameters of CF_3OH and CCl_3OH are very close and also close to those of methanol.

The transition state $CCl_3OH^{\neq}$, denoted by TS1Cl, describes the decomposition of CCl_3OH according to the reaction $CCl_3OH \rightarrow CCl_2O + HCl$. Despite the apparent similarity, the molecular structures of TS1Cl and TS1F show distinct differences in structural parameters. TS1Cl has a symmetry of C_1 point group. The C-Cl_1 contact distance of 2.46 Å is longer by 0.74 Å than the C–F_1 bond in the $CF_3OH^{\neq}$ structure. The O–H bond length is shorter by 0.13 Å compared with that in $CF_3OH^{\neq}$. The valence angles Cl–C–O of 82° and C–O–H of 97° differ distinctly from the F–C–O and C–O–H angles in TS1F. The relative total energy of $CCl_3OH^{\neq}$ of 33.9 kcal mol^{-1} with respect to CCl_3OH corresponds to the energy barrier for the thermal decomposition of CCl_3OH at 0 K.

The pre-reaction adduct $CCl_3OH...H_2O$ (MC1Cl) maintains the C_s symmetry of the CCl_3OH molecule. The geometrical parameters, especially bond lengths and bond angles, of this hydrogen-bonding complex are close to those in the isolated reactants CCl_3OH and H_2O. Only the O–H bond is longer by 0.02 Å and the C–O bond is 0.03 Å shorter than the corresponding bonds in CCl_3OH. The H–O contact distance of 1.72 Å is slightly shorter than in MC1F. The thermal stability of MC1Cl with respect to the reactants estimated at the G2 level is 8.5 kcal mol^{-1} at 0 K. This is almost half that of the heat of formation of MC1F from the reactants, $CF_3OH + H_2O$.

The transition state $(CCl_3OH..H_2O)^{\neq}$, denoted by TS2Cl, describes the decomposition of trichloromethanol accelerated by vapor water. The geometrical configuration of TS2Cl is similar to that of TS2F, but the lengths of the corresponding bonds differ considerably. The contact distances C...Cl_1 and O...H derived at the G2 level are 2.28 Å and 1.36 Å, respectively. A shift of H_2O in the direction of the abstracted chlorine atom Cl_1 only slightly changes the orientation of the CCl_3OH-skeleton of TS2Cl compared with CCl_3OH. The dihedral angle Cl_1–C–O–H of 60° of the MC1Cl structure decreases to 43° in TS2Cl. The relative G2-energy of TS2Cl toward the reactants $CCl_3OH + H_2O$ was calculated as 9.1 kcal mol^{-1} at 0 K.

The post-reaction adduct $CCl_2O...HCl...H_2O$, denoted by MC2Cl, is the most stable molecular structure in the $CCl_3OH + H_2O$ reaction system. The molecular complex MC2Cl is a loose structure with contact distances between the CCl_2O, HCl, and H_2O subunits of 3.63 Å, 1.79 Å, and 2.06 Å for C...Cl_1, $H_1...O_1$, and O...H, respectively. The dissociation energy of MC2Cl to the final reaction products is found to be 8.7 kcal mol^{-1} at 0 K.

The profiles of the potential energy surface calculated for the decomposition of CCl_3OH ($+H_2O$) are shown in Fig. 3.

Table 2 Molecular properties of the structures taking part in the reaction mechanism of the thermal decomposition of trichloromethanol [a)]

	CCl_3OH	TS1Cl	MC1Cl	TS2Cl	MC2Cl	CCl_2O
CO	1.3684	1.2773	1.3425	1.2477	1.2022	1.1949
OH	0.9781	1.1215	1.0005	1.3645	2.0649	
CCl_1	1.7916	2.4629	1.8118	2.2792	3.6272	1.7447
CCl_2	1.7916	1.7062	1.8118	1.7443	1.7329	1.7447
CCl_3	1.7586	1.7002	1.7613	1.7696	1.7314	
O_1H			1.7247	1.1079	0.9744	
O_1H_1			0.9723	1.0350	1.7949	
O_1H_0			0.9723	0.9793	0.9709	
COH	108.1514	97.4696	108.4503	112.7419	124.9084	
Cl_1CO	111.0518	82.3137	111.7225	104.9041	82.2081	123.8843
Cl_2CO	111.0518	120.5714	111.7225	117.6260	123.5627	123.8843
Cl_3CO	106.4187	119.6577	108.1472	118.4298	123.2232	
OHO_1			168.4415	158.2192	147.5631	
HO_1H_1			107.1772	96.2210	100.6430	
HO_1H_0			107.1772	107.4380	104.7323	
Cl_1COH	60.1553	5.1592	59.7877	42.7587	−47.7625	
Cl_2COH	−60.1553	94.5080	−59.7877	154.0591	33.3557	
Cl_3COH	180.0000	−110.9961	180.0000	−66.0320	−147.6460	
O_1HOC			0.0000	−51.1168	65.3616	
H_1O_1HO			55.9729	20.9677	−13.7080	
H_0O_1HO			−55.9729	−88.3072	101.0634	
υ_1	234	1611 i [b)]	48	556 i [b)]	6	295
υ_2	245	72	61	60	14	445
υ_3	324	219	79	109	28	565
υ_4	342	282	165	148	31	581
υ_5	393	320	237	199	90	878
υ_6	414	424	253	232	135	1856
υ_7	526	539	276	304	157	
υ_8	798	593	298	310	243	
υ_9	802	961	341	372	298	
υ_{10}	1143	1185	393	445	346	
υ_{11}	1297	1399	416	529	445	
υ_{12}	3619	2612	521	605	455	
υ_{13}			741	701	542	
υ_{14}			785	814	576	
υ_{15}			805	984	587	
υ_{16}			1178	1275	903	
υ_{17}			1373	1571	1636	
υ_{18}			1625	1585	1825	
υ_{19}			3396	1654	2650	
υ_{20}			3629	3238	3625	
υ_{21}			3728	3642	3725	
E_0(G2)	−1492.98743	−1492.93343	−1569.33306	−1569.30504	−1569.34908	−1032.66305

[a)] units as in Table 1.
[b)] the unscaled MP2/6–31G(d) vibrational frequencies (cm^{-1})

The thermal decomposition of CCl_3OH is an exothermic reaction at all temperatures considered in this study. The calculated reaction enthalpy of -9.9 kcal mol^{-1} at 0 K changes to -8.9 kcal mol^{-1} at ambient temperature. The energy barrier for reaction (3) calculated at the G2 level is high, 33.9 kcal mol^{-1}, at 0 K. This is 3.7 kcal mol^{-1} less than the analogous reaction of CF_3OH. A more complex reaction mechanism is postulated when the decomposition of CCl_3OH proceeds in the presence of water. The approach of the H_2O molecule to CCl_3OH leads to the formation of the MC1Cl intermediate complex. The calculated binding energy between water and alcohol of 8.5 kcal mol^{-1} is 7.0 kcal mol^{-1} less than that derived for $H_2O...CF_3OH$ in MC1F. The reaction path leads through the transition state TS2Cl toward another molecular complex, MC2Cl, which finally dissociates into reaction products. The threshold

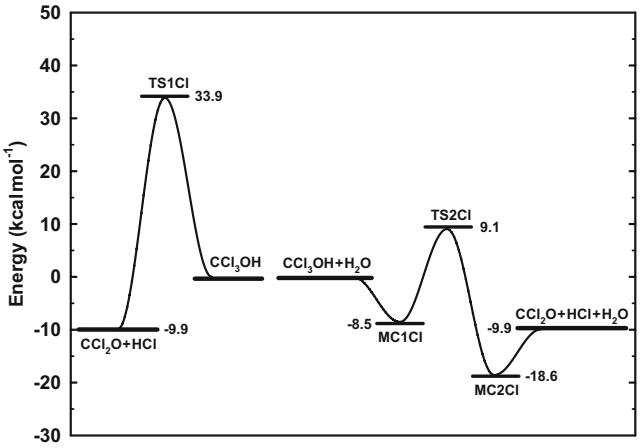

Fig. 3 Schematic energy profile for the decomposition of CCl_3OH in the absence (left side) and presence (right side) of water. The energies are calculated at the G2 level including zero-point energy corrections

energy for this pathway toward the reactants is calculated as 9.1 kcal mol^{-1}. The reaction barrier is then 2.4 kcal mol^{-1} lower than that for the $CF_3OH + H_2O$ reaction system.

Thermal decomposition of CBr_3OH

The molecular properties of the molecular structures taking part in the reaction mechanism of the decomposition of CBr_3OH in the presence of H_2O are given in Table 3. A staggered conformation of C_s symmetry was found to be the most stable molecular structure of CBr_3OH. Except for the C-Br bond lengths, the geometrical parameters of CBr_3OH are close to their analogues in the CCl_3OH and CF_3OH molecules.

The saddle point $CBr_3OH^{\neq}$, denoted by TS1Br, for the thermal decay of CBr_3OH is a molecular structure of C_1 symmetry, like TS1Cl. All interatomic distances in $CBr_3OH^{\neq}$ are systematically longer than in $CF_3OH^{\neq}$ and $CCl_3OH^{\neq}$, whereas the angle parameters are indeed equivalent to those in $CCl_3OH^{\neq}$. The energy barrier for the decomposition $CBr_3OH \rightarrow CBr_2O + HBr$ calculated at the G2 level is 31.7 kcal mol^{-1} at 0 K.

The pre-reaction adduct $CBr_3OH...H_2O$, denoted by MC1Br, has a symmetry of C_s point group. The geometrical parameters of both the CBr_3OH and H_2O subunits of MC1Br are close to those in the isolated reactants. Only the O–H bond is 0.03 Å longer and the C–O bond 0.03 Å shorter than the corresponding bonds in CBr_3OH. The contact distance of $H–O_1$ of 1.69 Å is slightly shorter than in the MC1Cl and MC1F intermediate complexes. The formation of MC1Br is a less exothermic process than the formation of MC1Cl and MC1F.

The transition state $(CBr_3OH..H_2O)^{\neq}$, denoted by TS2Br, is a critical structure in the description of the decomposition of tribromomethanol in the presence of water. The molecular structure of TS2Br shows similarity to TS2Cl. This is especially visible in the angular parameters. However, except for the H–O, $H–O_1$, and C–O bond lengths, the bonds of TS2Br are considerably enlarged compared with their counterparts in TS2Cl. The $C...Br_1$, $Br_1...H_1$, and $O_1...H$ contact distances derived at the G2 level are 2.39, 2.05, and 1.43 Å, respectively. The dihedral angle $Br_1–C–O–H$ of 60° at MC1Br structure is reduced to 45.5° in TS2Cl. The energy barrier for the reaction $CBr_3OH + H_2O$ is estimated to be 11.5 kcal mol^{-1} at 0 K.

The post-reaction adduct $CBr_2O...HBr...H_2O$, denoted by MC2Br, is a loose structure with contact distances between the CBr_2O, HBr, and H_2O subunits of 3.36, 1.80, and 2.14 Å for C...Br, H...O, and O...H, respectively. The molecular complex MC2Br is the most stable structure in the $CBr_3OH + H_2O$ reaction system. Its dissociation energy to the final reaction products is found to be 5.9 kcal mol^{-1} at 0 K.

The mechanism of the thermal decomposition of CBr_3OH ($+H_2O$) can be analyzed in terms of the profiles of the potential energy surface, which are shown in Fig. 4. The thermal decomposition of CBr_3OH is the most exothermic process among the reactions under investigation. However, the calculated values of the reaction's enthalpy are very close to those obtained for the decay of CCl_3OH. The height of the energy barrier for the reaction $CBr_3OH \rightarrow CBr_2O + HBr$ is high, 31.7 kcal mol^{-1}, but lower than those derived for the decomposition of CF_3OH and CCl_3OH. If the decomposition of CBr_3OH occurs in the presence of H_2O, the reaction mechanism is complex and consists of three elementary steps. Intermediate complexes are formed during the reaction. The thermal stability of the molecular complexes with respect to the reactants (MC1X) and products (MC2X) decreases when X changes in the series from F to Br. The reaction $CBr_3OH + H_2O$ is related to the lowest energy barrier and is expected to be the fastest process among the reactions analyzed.

Rate constant calculations

The rate constants for the thermal decomposition of perhalogenated methanols were analyzed in terms of conventional transition state theory. The calculated energy barrier for the reactions $CX_3OH \rightarrow COX_2 + HX$ (where X = F, Cl, and Br) are high, over 30 kcal mol^{-1}. A reaction with a high energy barrier is usually characterized by a significant tunneling effect, which is represented in the rate constant calculation by the tunneling correction factor κ_W as:

$$k = \kappa_W \, k_{TST}. \quad (7)$$

Including the tunneling effect may distinctly improve the values of calculated rate constants, especially at low temperatures. A number of different kinds of tunneling corrections have been evaluated by Garrett and Truhlar [41], who found

Table 3 Molecular properties of the structures taking part in the reaction mechanism of the thermal decomposition of tribromomethanol [a)]

	CBr_3OH	TS1Br	MC1Br	TS2Br	MC2Br	CBr_2O
CO	1.3624	1.2710	1.3315	1.2407	1.1982	1.1900
OH	0.9801	1.1504	1.0091	1.4279	2.1358	
CBr_1	1.9775	2.5714	2.0079	2.3891	3.3639	1.9309
CBr_2	1.9775	1.8919	2.0079	1.9396	1.9197	1.9309
CBr_3	1.9364	1.8831	1.9372	1.9775	1.9099	
O_1H			1.6941	1.0811	0.9743	
O_1H_1			0.9742	1.0417	1.7972	
O_1H_0			0.9742	0.9805	0.9716	
COH	107.9101	98.3400	108.1147	111.0343	111.8381	
Br_1CO	111.4618	83.4133	112.3163	106.9340	94.0399	124.1137
Br_2CO	111.4618	120.7480	112.3163	118.0819	123.1555	124.1137
Br_3CO	107.0317	120.0365	109.2515	117.8694	123.9868	
OHO_1			163.4107	157.8613	143.1249	
HO_1H_1			102.4967	97.7460	101.1046	
HO_1H_0			102.4967	106.9005	104.4710	
Br_1COH	60.0759	5.1414	59.4155	45.5070	−52.2451	
Br_2COH	−60.0759	−95.0590	−59.4155	158.5845	34.9541	
Br_3COH	180.0000	110.7385	180.0000	−64.1174	−145.6005	
O_1HOC			0.0000	−53.8525	74.7250	
H_1O_1HO			53.8987	23.6367	−25.3962	
H_0O_1HO			−53.8987	−85.9707	87.8742	
υ_1	148	1780 i [b)]	61	355 i [b)]	8	179
υ_2	151	45	77	49	24	347
υ_3	211	132	138	72	39	410
υ_4	264	192	143	110	51	515
υ_5	308	240	150	143	94	751
υ_6	368	340	173	192	119	1861
υ_7	398	430	209	220	135	
υ_8	693	529	264	301	180	
υ_9	697	825	332	303	206	
υ_{10}	1127	1165	338	390	313	
υ_{11}	1285	1378	373	423	353	
υ_{12}	3608	2512	400	521	415	
υ_{13}			663	604	435	
υ_{14}			705	776	511	
υ_{15}			772	826	538	
υ_{16}			1166	1401	770	
υ_{17}			1374	1554	1634	
υ_{18}			1630	1590	1829	
υ_{19}			3360	1659	2350	
υ_{20}			3622	3187	3624	
υ_{21}			3718	3617	3724	
E_0(G2)	−7831.48792	−7831.43746	−7907.83276	−7907.80957	−7907.84633	−5258.33155

[a)] units as in Table 1.
[b)] the unscaled MP2/6–31G(d) vibrational frequencies (cm^{-1})

that the simplest, that of Wigner [30, 41], was also often the most accurate. We adopt the Wigner correction:

$$\kappa_W \cong 1 - \frac{1}{24}\left(\frac{h\nu^{\neq}}{k_B T}\right)^2 \quad (8)$$

where $\upsilon^{\neq}$ is the imaginary frequency of the transition state. The magnitude of the imaginary frequency is related to the thickness of the potential barrier in the vicinity of the transition state along the reaction coordinate. The tunneling correction factor depends sensitively on the imaginary frequency used in the calculation, whereas the imaginary frequencies depend significantly on the level of calculations. Therefore we decided to evaluate the tunneling factors with the imaginary frequencies obtained in the geometry optimization performed at a higher level of theory, i.e., from MP2/6–31G(d) calculations.

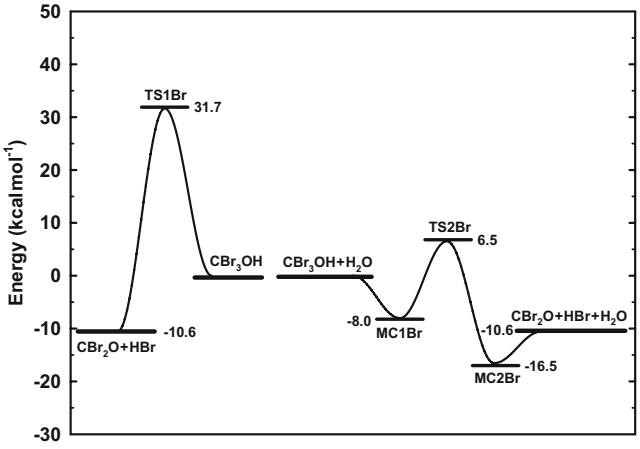

Fig. 4 Schematic energy profile for the decomposition of CBr_3OH in the absence (left side) and presence (right side) of water. The energies are calculated at the G2 level including zero-point energy corrections

Values of the calculated rate constants are given in Tables 4, 5, and 6. The superscript of the rate constant denote the order of the reaction, i.e., $k^{(1)}$ is the rate constant for the first-order decomposition of CX_3OH, $k^{(2)}$ for the second-order reaction $CX_3OH + H_2O$, etc. The differences in height of the energy barriers for the decomposition of CX_3OH are reflected in the calculated values of the first-order rate constants, $k^{(1)}$. Values of 3.3×10^{-14}, 3.8×10^{-11}, and 1.9×10^{-9} s^{-1} were derived at room temperature for the decay of CF_3OH, CCl_3OH, and CBr_3OH, respectively. The atmospheric lifetimes of CX_3OH corresponding to these values of $k^{(1)}$ are many orders of magnitude greater than the upper limits measured experimentally. This strongly suggests that the decomposition of CX_3OH in the atmosphere must then proceed according to a different and considerably more efficient reaction mechanism.

The reaction mechanism, which takes into consideration the role of a water molecule in the decomposition of CX_3OH, consists of three consecutive processes with the pathway:

$$CX_3OH + H_2O \leftrightarrows CX_3OH\ldots H_2O \leftrightarrows CX_2O\ldots HX\ldots \quad (9)$$
$$H_2O \rightarrow CX_2O + HF + H_2O.$$

The first and the third elementary processes are unimolecular dissociation/recombination, while the second step is related to an energy barrier. Bimolecular reactions, which involve the formation of intermediate molecular complexes, often show unusual temperature and pressure dependence [42]. In the case of loosely bound intermediates, their collisional stabilization can, in a first approximation, be omitted in the description of the reaction rate. A method for the rate constant calculation for a bimolecular reaction which proceeds through the formation of two weakly bound intermediate complexes has been successfully applied to describe the kinetics of the H-abstraction from methanol [35–37]. The general equation, which takes into account the rotational energy, is derived from RRKM theory. According to this formalism, the rate constant $k^{(2)}_{exact}$ for the multi-step decomposition of CX_3OH can be expressed as:

$$k^{(2)}_{exact} = \frac{z}{hQ_AQ_B}\int_{V_{TS2X}}^{\infty}\sum_J W_{MC1X}(E,J)\times\frac{W_{TS2X}(E,J)}{W_{MC1X}(E,J)+W_{TS2X}(E,J)}\times \frac{W_{MC2X}(E,J)}{W_{MC2X}(E,J)+W_{TS2X}(E,J)}\times\exp(-E/RT)dE, \quad (10)$$

where Q_A and Q_B are the partition functions of CX_3OH and H_2O, respectively, with the center of mass partition function factored out of the product Q_{AB}, and included in z together with the partition functions of those inactive degrees of

Table 4 The rate constants calculated for the unimolecular ($k^{(1)}$) and the bimolecular, accelerated by water ($k^{(2)}$) decomposition of CF_3OH

T (K)	$k^{(1)}_{TST}$ (s^{-1})	$\kappa^{(1)}$ a)	$k^{(1)}$ (s^{-1})	$k^{(2)}_{TST}$ ($cm^3molecule^{-1}s^{-1}$)	$\kappa^{(2)}$ a)	$k^{(2)}$ ($cm^3molecule^{-1}s^{-1}$)	$k^{(2)}_{exact}$ ($cm^3molecule^{-1}s^{-1}$)
200	1.19×10^{-28}	7.668	9.08×10^{-28}	1.12×10^{-25}	2.193	2.46×10^{-25}	2.46×10^{-25}
250	2.36×10^{-20}	5.267	1.24×10^{-19}	3.39×10^{-23}	1.764	5.97×10^{-23}	5.97×10^{-23}
300	8.26×10^{-15}	3.963	3.28×10^{-14}	1.61×10^{-21}	1.530	2.47×10^{-21}	2.47×10^{-21}
350	7.65×10^{-11}	3.177	2.43×10^{-10}	2.68×10^{-20}	1.390	3.72×10^{-20}	3.72×10^{-20}
400	7.30×10^{-8}	2.667	1.95×10^{-7}	2.29×10^{-19}	1.298	2.97×10^{-19}	2.97×10^{-19}
450	1.53×10^{-5}	2.317	3.54×10^{-5}	1.26×10^{-18}	1.236	1.56×10^{-18}	1.56×10^{-18}
500	1.11×10^{-3}	2.067	2.29×10^{-3}	5.07×10^{-18}	1.191	6.04×10^{-18}	6.03×10^{-18}
600	6.88×10^{-1}	1.741	1.20×10^{0}	4.37×10^{-17}	1.133	4.95×10^{-17}	4.95×10^{-17}
700	6.90×10^{1}	1.544	1.07×10^{2}	2.18×10^{-16}	1.097	2.39×10^{-16}	2.39×10^{-16}
800	2.20×10^{3}	1.417	3.12×10^{3}	7.68×10^{-16}	1.075	8.26×10^{-16}	8.24×10^{-16}
900	3.28×10^{4}	1.329	4.36×10^{4}	2.14×10^{-15}	1.059	2.27×10^{-15}	2.26×10^{-15}
1000	2.87×10^{5}	1.267	3.63×10^{5}	5.03×10^{-15}	1.048	5.28×10^{-15}	5.26×10^{-15}
1500	1.99×10^{8}	1.119	2.22×10^{8}	8.89×10^{-14}	1.021	9.08×10^{-14}	9.06×10^{-14}
2000	5.42×10^{9}	1.067	5.78×10^{9}	5.00×10^{-13}	1.012	5.06×10^{-13}	5.05×10^{-13}
3000	1.53×10^{11}	1.030	1.57×10^{11}	4.17×10^{-12}	1.005	4.19×10^{-12}	4.13×10^{-12}

a) Wigner tunneling correction factor calculated for the imaginary frequency of the respective transition state from Table 1.

Table 5 The rate constants calculated for the unimolecular ($k^{(1)}$) and the bimolecular, accelerated by water ($k^{(2)}$) decomposition of CCl_3OH

T (K)	$k^{(1)}_{TST}$ (s^{-1})	$\kappa^{(1)}$ a)	$k^{(1)}$ (s^{-1})	$k^{(2)}_{TST}$ ($cm^3molecule^{-1}s^{-1}$)	$\kappa^{(2)}$ a)	$k^{(2)}$ ($cm^3molecule^{-1}s^{-1}$)	$k^{(2)}_{exact}$ ($cm^3molecule^{-1}s^{-1}$)
200	2.99×10^{-24}	6.594	1.97×10^{-23}	6.85×10^{-23}	1.671	1.15×10^{-22}	1.14×10^{-22}
250	1.01×10^{-16}	4.580	4.63×10^{-16}	7.06×10^{-21}	1.430	1.01×10^{-20}	1.01×10^{-20}
300	1.08×10^{-11}	3.486	3.77×10^{-11}	1.63×10^{-19}	1.298	2.12×10^{-19}	2.12×10^{-19}
350	4.27×10^{-8}	2.827	1.21×10^{-7}	1.61×10^{-18}	1.219	1.96×10^{-18}	1.96×10^{-18}
400	2.14×10^{-5}	2.399	5.13×10^{-5}	9.22×10^{-18}	1.168	1.08×10^{-17}	1.08×10^{-17}
450	2.70×10^{-3}	2.105	5.69×10^{-3}	3.70×10^{-17}	1.133	4.19×10^{-17}	4.19×10^{-17}
500	1.30×10^{-1}	1.895	2.46×10^{-1}	1.15×10^{-16}	1.107	1.28×10^{-16}	1.28×10^{-16}
600	4.35×10^{1}	1.622	7.05×10^{1}	6.71×10^{-16}	1.075	7.21×10^{-16}	7.21×10^{-16}
700	2.77×10^{3}	1.457	4.03×10^{3}	2.52×10^{-15}	1.055	2.66×10^{-15}	2.65×10^{-15}
800	6.26×10^{4}	1.350	8.45×10^{4}	7.15×10^{-15}	1.042	7.45×10^{-15}	7.44×10^{-15}
900	7.09×10^{5}	1.276	9.05×10^{5}	1.68×10^{-14}	1.033	1.74×10^{-14}	1.73×10^{-14}
1000	4.95×10^{6}	1.224	6.06×10^{6}	3.45×10^{-14}	1.027	3.54×10^{-14}	3.53×10^{-14}
1500	1.72×10^{9}	1.099	1.89×10^{9}	3.99×10^{-13}	1.012	4.04×10^{-13}	4.01×10^{-13}
2000	3.25×10^{10}	1.056	3.44×10^{10}	1.81×10^{-12}	1.007	1.82×10^{-12}	1.79×10^{-12}
3000	6.28×10^{11}	1.025	6.43×10^{11}	1.20×10^{-11}	1.003	1.21×10^{-11}	1.14×10^{-11}

a) Wigner tunneling correction factor calculated for the imaginary frequency of the respective transition state from Table 2.

freedom which are not considered by the sums of the states under the integral. V_{TS2X} is the threshold energy toward the reactants $CX_3OH + H_2O$ and $W_{TS2X}(E,J)$, $W_{MC1X}(E,J)$, and $W_{MC2X}(E,J)$ denote the sum of the states at energy less than or equal to E and with angular momentum J for the transition state TS2X and the activated complexes for the unimolecular dissociations of MC1X and MC2X, respectively. All computational effort is then related to calculation of the sum of the states, $W(E,J)$. This calculation depends on the level at which the conservation of angular momentum is considered and is discussed in detail in refs. [35, 36].

The dominant contribution to the rate constant is given by the states with energy E not higher than $V_{TS2X} + 3RT$. In the case of a sizable (compared with RT) energy barrier V_{TS2X}, the value of the product of the microcanonical branching fractions at an energy slightly higher than V_{TS2X} becomes close to unity

$$\frac{W_{MC1X}(E,J)}{W_{MC1X}(E,J)+W_{TS2X}(E,J)}\times\frac{W_{MC2X}(E,J)}{W_{MC2X}(E,J)+W_{TS2X}(E,J)}\cong 1 \quad (11)$$

because the values of $W_{TS2X}(E,J)$ are negligibly small compared with both $W_{MC1X}(E,J)$ and $W_{MC2X}(E,J)$. This

Table 6 The rate constants calculated for the unimolecular ($k^{(1)}$) and the bimolecular, accelerated by water ($k^{(2)}$) decomposition of CBr_3OH

T (K)	$k^{(1)}_{TST}$ (s^{-1})	$\kappa^{(1)}$ a)	$k^{(1)}$ (s^{-1})	$k^{(2)}_{TST}$ ($cm^3molecule^{-1}s^{-1}$)	$\kappa^{(2)}$ a)	$k^{(2)}$ ($cm^3molecule^{-1}s^{-1}$)	$k^{(2)}_{exact}$ ($cm^3molecule^{-1}s^{-1}$)
200	9.26×10^{-22}	7.754	7.18×10^{-21}	3.99×10^{-20}	1.272	5.07×10^{-20}	5.07×10^{-20}
250	9.86×10^{-15}	5.323	5.25×10^{-14}	1.14×10^{-18}	1.174	1.33×10^{-18}	1.33×10^{-18}
300	4.83×10^{-10}	4.002	1.93×10^{-9}	1.11×10^{-17}	1.121	1.25×10^{-17}	1.24×10^{-17}
350	1.09×10^{-6}	3.205	3.49×10^{-6}	5.90×10^{-17}	1.089	6.42×10^{-17}	6.39×10^{-17}
400	3.58×10^{-4}	2.688	9.62×10^{-4}	2.13×10^{-16}	1.068	2.28×10^{-16}	2.26×10^{-16}
450	3.25×10^{-2}	2.334	7.58×10^{-2}	5.97×10^{-16}	1.054	6.29×10^{-16}	6.24×10^{-16}
500	1.20×10^{0}	2.081	2.49×10^{0}	1.39×10^{-15}	1.043	1.45×10^{-15}	1.44×10^{-15}
600	2.69×10^{2}	1.750	4.70×10^{2}	5.26×10^{-15}	1.030	5.42×10^{-15}	5.36×10^{-15}
700	1.29×10^{4}	1.551	1.99×10^{4}	1.45×10^{-14}	1.022	1.48×10^{-14}	1.46×10^{-14}
800	2.34×10^{5}	1.422	3.33×10^{5}	3.26×10^{-14}	1.017	3.31×10^{-14}	3.25×10^{-14}
900	2.25×10^{6}	1.334	3.00×10^{6}	6.38×10^{-14}	1.013	6.46×10^{-14}	6.30×10^{-14}
1000	1.37×10^{7}	1.270	1.74×10^{7}	1.13×10^{-13}	1.011	1.14×10^{-13}	1.11×10^{-13}
1500	3.19×10^{9}	1.120	3.58×10^{9}	8.45×10^{-13}	1.005	8.49×10^{-13}	7.84×10^{-13}
2000	4.96×10^{10}	1.068	5.30×10^{10}	3.07×10^{-12}	1.003	3.08×10^{-12}	2.66×10^{-12}
3000	7.86×10^{11}	1.030	8.09×10^{11}	1.64×10^{-11}	1.001	1.65×10^{-11}	1.21×10^{-11}

a) Wigner tunneling correction factor calculated for the imaginary frequency of the respective transition state from Table 3.

enables one to evaluate the integral, which is, by definition, simply the TST rate constant $k^{(2)}$

$$\frac{z}{hQ_AQ_B}\int_{V_{TS2X}}^{\infty}\sum_{J}W_{TS2X}(E,J)\times\exp(-E/RT)dE=k^{(2)}. \quad (12)$$

The rate of the reaction is then determined by the height of the energy taken as the energy difference between the reactants and TS2X, whereas the intermediates, MC1X and MC2X, disappear from the reaction mechanism. Thus the rate constant $k^{(2)}$ represents an upper limit of the rate constant $k^{(2)}_{exact}$ for the multi-step reaction mechanism. Analysis of the data in Table 4 shows that the rate constants $k^{(2)}$ obtained from conventional transition state theory are very good approximations of the exact rate constants $k^{(2)}_{exact}$ calculated from Eq. (10) taking into account the formation of pre- and post-reaction molecular complexes. The difference between $k^{(2)}$ and $k^{(2)}_{exact}$ for CF_3OH/CCl_3OH + H_2O reactions are, at temperatures below 1000 K, practically negligible, and even at 3000 K only slightly exceed 1% and 5% for CF_3OH and CCl_3OH, respectively. The transition state theory reliably describes the kinetics of the CF_3OH + H_2O and CCl_3OH + H_2O reactions except at extremely high temperatures. This is due to the relatively higher energy barrier for these reactions. In the case of CBr_3OH + H_2O, the differences between $k^{(2)}$ and $k^{(2)}_{exact}$ are more visible and exceed 3%, 14%, and 27% at 1000 K, 2000 K, and 3000 K, respectively. Despite these differences, the conventional transition state theory is a useful tool in describing reaction kinetics, especially if one takes into consideration the precision of kinetic measurements.

The height of the energy barrier is clearly the major factor determining the magnitude of the rate constant and its dependence on temperature. The presence of water promotes the elimination of HX from the CX_3OH molecule, which results in a reduction of the energy barrier compared with the simple decomposition of CX_3OH. The differences in the heights of the energy barriers for the reactions under investigation reach 25 kcal mol^{-1}. The temperature dependence of the calculated rate constants $k^{(2)}$ is therefore considerably weaker than that of $k^{(1)}$. The lowest energy barrier in the CX_3OH + H_2O reaction systems of 6.5 kcal mol^{-1} occurs in the reaction of tribromomethanol with a water molecule. The calculated rate constant $k^{(2)}$ for this reaction is the highest one, with 1.2×10^{-17} $cm^3molecule^{-1}s^{-1}$ at room temperature. On the other hand, the reaction of CF_3OH + H_2O proceeds through the highest energy barrier, of 11.2 kcal mol^{-1}. The calculated value of $k^{(2)}$ for this reaction, i.e., 2.5×10^{-21} $cm^3molecule^{-1}s^{-1}$ at 300 K, is four orders of magnitude lower than that obtained for the reaction CBr_3OH + H_2O. With an energy barrier of 9.1 kcal mol^{-1}, the decomposition of CCl_3OH in the presence of water proceeds distinctly faster than that of CF_3OH and much more slowly than that of CBr_3OH. The rate of CCl_3OH + H_2O is characterized by a value of $k^{(2)}$ of 2.1×10^{-19} $cm^3molecule^{-1}s^{-1}$ at room temperature.

The atmospheric lifetime τ of the species describes the rate of decay of this molecule with respect to a given reaction under atmospheric conditions. The lifetime τ can be considered as the average length of time of a species in the atmosphere [2]. The value of τ is directly related to the rate constant and to the concentrations of any other compounds involved in the reaction in the atmosphere. The atmospheric lifetime of CX_3OH with respect to its thermal decomposition reaction can be expressed in the forms: $\tau = 1/k^{(1)}$ and $\tau = 1/k^{(2)}$ $[H_2O]$ for the first- and second-order (CX_3OH + H_2O) decomposition of the alcohol, respectively. At room temperature, the calculated values of τ for CX_3OH with respect to the thermal decomposition reaction $CX_3OH \rightarrow CX_2O + HX$ are very high, i.e., 10^6, 840, and 16 years, for CF_3OH, CCl_3OH, and CBr_3OH, respectively. These are a few orders of magnitude greater than the experimental estimates. In the presence of water vapor, the decomposition of the halogenated alcohols proceeds considerably faster. In consequence, the atmospheric lifetime of CX_3OH with respect to the water-accelerated decomposition is incomparably shorter. An atmospheric water concentration of 10^{17} molecules cm^{-3} [2] is typical of altitudes below 5 km, and this value was used in our calculations. Values of the lifetime of CX_3OH with respect to the homogenous reaction with H_2O calculated at room temperature are 68 min, 47 s, and 0.8 s for CF_3OH, CCl_3OH, and CBr_3OH, respectively. Water vapor accelerates the decomposition of CX_3OH by more than nine orders of magnitude at room temperature.

The measured overall rate constant for the decomposition of CF_3OH covers the range of $(0.4 - 6.0)\times10^{-4}$ s^{-1} [5, 10, 11], which corresponds to a lifetime of CF_3OH of 0.5–7 hr. Molecules of CCl_3OH undergo decomposition much faster than those of CF_3OH. The upper limit of the rate constant for the decay of CCl_3OH was calculated as 1.05×10^{-2} s^{-1} [20], so the lifetime of CCl_3OH under similar conditions is considerably shorter of 95 s. This confirms the reliability of our theoretical analysis despite the simplicity of the computational model used.

Summary

The main aim of the present study is related to a further understanding of the atmospheric chemistry of CX_3OH alcohols. Theoretical investigations based on ab initio calculations of the reaction systems at the G2 level were performed to gain insight into the role played by water molecules in the homogeneous decay of CX_3OH molecules,

especially for the case of CF_3OH because experimental data are accessible only for its decomposition. The results of these calculations show that the reaction $CF_3OH \rightarrow CF_2O + HF$ is almost thermoneutral, but the sign of the reaction enthalpy depends on temperature.

The energy barriers derived at the G2 level for the unimolecular and water-accelerated decomposition of CF_3OH are distinctly lower than those reported in literature obtained at different levels of theory [4, 8, 13]. However, considering an activation energy of 37.6 kcal mol^{-1}, the unimolecular path is unlikely and related to a negligibly slow reaction rate. Results of calculations show that the mechanism of decomposition of CX_3OH in the presence of water is complex and that the reaction proceeds with the formation of pre- and post-reaction adducts. The energy barrier of 11.5 kcal mol^{-1} obtained in this study at the G2 level for the water-mediated decay of CF_3OH is lower than those calculated at other levels of theory. This suggests that the homogenous decomposition of CF_3OH in the presence of water vapor may proceed considerably faster than was previously estimated. The calculated rate constant may reach a value of 2.5×10^{-21} $cm^3molecule^{-1}s^{-1}$ at room temperature, which yields a lifetime of CF_3OH with respect to the homogeneous reaction with H_2O vapor of 1 h at the assumed H_2O concentration of 10^{17} $cm^3molecule^{-1}s^{-1}$. At the lower temperatures more typical of the atmosphere, the predicted lifetime will obviously be greater, but will remain comparable to the upper limit of the experimental estimates.

The heterogeneous reactions between CX_3OH and H_2O cause, however, the major loss of atmospheric CX_3OH. The influence of multiple water molecules in stabilizing the transition state should lead to a further lowering the reaction barrier. The heterogeneous reaction may also be accelerated by a high local water concentration when the decomposition proceeds on a water surface, such as clouds and raindrops.

Homogeneous decomposition of CX_3OH cannot be competitive with the heterogeneous reaction under atmospheric conditions. However, the relatively strong association between CX_3OH and H_2O in the formed pre-reaction adducts suggests that CX_3OH may readily bond with water and these interactions may play a role in further promoting the elimination of HX from CX_3OH. Therefore, a reliable assessment of the role of homogeneous water-accelerated decomposition of CX_3OH molecules requires direct kinetic measurements to provide an accurate estimate of the rate constants for the investigated reactions.

Acknowledgment The authors are grateful for the support of the Atmospheric Dispersion Project funded by the National Oceanic and Atmospheric Administration through the U.S. Department of Commerce (Silver Spring, MD; Contract #NA06OAR4600192). The Wroclaw Center of Networking and Supercomputing is acknowledged for a generous allotment of computer time.

References

1. Wayne RP, Poulet G, Biggs P, Burrows JP, Cox RA, Crutzen PJ, Hayman GD, Jenkin ME, LeBras G, Moortgat GK, Platt U, Schindler RN (1995) Atmos Environ 29:2677–2881
2. Finnlayson-Pitts BJ, Pitts JN Jr (2000) Chemistry of the upper and lower atmosphere. Academic, San Diego
3. Wallington TJ, Dagaut P, Kurylo MJ (1992) Chem Rev 92:667–710
4. Francisco JS (1991) Chem Phys 150:19–27
5. Sehested J, Wallington TJ (1993) Environ Sci Technol 27:146–152
6. Bock CW, Trachtman M, Niki H, Mains GJ (1994) J Phys Chem 98:7976–7980
7. Wallington TJ, Schneider WF (1994) Environ Sci Technol 28:1198–1200
8. Francisco JS (1994) Chem Phys Lett 218:401–405
9. Schneider WF, Wallington TJ, Minschwaner K, Stahlberg EA (1995) Environ Sci Technol 29:247–250
10. Huey LG, Hanson DR, Lovejoy ER (1995) J Geophys Res 100:18771–18774
11. Bednarek G, Kohlmann JP, Saathoff H, Zellner R (1995) Z Phys Chem (Munich) 188:1–15
12. Lovejoy ER, Huey LG, Hanson DR (1995) J Geophys Res 100:18775–18780
13. Schneider WF, Wallington TJ, Huie RE (1996) J Phys Chem 100:6097–6103
14. Kim SJ, Song HS (1999) Bull Korean Chem Soc 20:1493–1500
15. Brudnik K, Jodkowski JT, Ratajczak E, Venkatraman R, Nowek A, Sullivan RH (2001) Chem Phys Lett 345:435–444
16. Brudnik K, Jodkowski JT, Ratajczak E (2003) J Mol Struct 656:333–339
17. Brudnik K, Jodkowski JT, Ratajczak E (2003) Bull Pol Acad Sci, Chem 51:77–91
18. Fernández LE, Varetti EL (2003) J Mol Struct (Theochem) 629:175–183
19. Tyndall GS, Wallington TJ, Hurley MD, Schneider WF (1993) J Phys Chem 97:1576–1582
20. Wallington TJ, Schneider WF, Barnes I, Becker KH, Sehested J, Nielsen OJ (2000) Chem Phys Lett 322:97–102
21. Schnell M, Mühlhäuser M, Peyerimhoff SD (2002) Chem Phys Lett 361:1–7
22. Sun H, Bozzelli JW (2001) J Phys Chem A 105:4504–4516
23. Brudnik K, Jodkowski JT, Nowek A, Leszczynski J (2007) Chem Phys Lett 435:194–200
24. Wallington TJ, Hurley MD, Schneider WF, Sehested J, Nielsen OJ (1993) J Phys Chem 97:7606–7611
25. Vöhringer-Martinez E, Hansmann B, Hernandez H, Francisco JS, Troe J, Abel B (2007) Science 315:497–501
26. Garrett BC (2004) Science 303:1146–1147
27. Takahashi K, Kramer ZC, Vaida V, Skodje RT (2007) Phys Chem Chem Phys 9:3864–3871
28. Frisch MJ, Trucks GW, Schlegel HB, Scuseria GE, Robb MA, Cheeseman JR, Montgomery JA Jr, Vreven T, Kudin KN, Burant JC, Millam JM, Iyengar SS, Tomasi J, Barone V, Mennucci B, Cossi M, Scalmani G, Rega N, Petersson GA, Nakatsuji H, Hada M, Ehara M, Toyota K, Fukuda R, Hasegawa J, Ishida M, Nakajima T, Honda Y, Kitao O, Nakai H, Klene M, Li X, Knox JE, Hratchian HP, Cross JB, Adamo C, Jaramillo J, Gomperts R, Stratmann RE, Yazyev O, Austin AJ, Cammi R, Pomelli C, Ochterski JW, Ayala PY, Morokuma K, Voth GA, Salvador P, Dannenberg JJ, Zakrzewski VG, Dapprich S, Daniels AD, Strain MC, Farkas O, Malick DK, Rabuck AD, Raghavachari K, Foresman JB, Ortiz JV, Cui Q, Baboul AG, Clifford S, Cioslowski J, Stefanov BB, Liu G, Liashenko A, Piskorz P, Komaromi I, Martin RL, Fox DJ, Keith T, Al-Laham MA, Peng CY, Nanayakkara A, Challacombe M, Gill PMW, Johnson B, Chen W, Wong MW, Gonzalez C, Pople JA (2003) Gaussian 03, Revision B.03. Gaussian, Inc, Pittsburgh PA

29. Curtiss LA, Raghavachari K, Trucks GW, Pople JA (1991) J Chem Phys 94:7221–7230
30. Johnston HS (1966) Gas-phase reaction rate theory. The Ronald Press Co, New York
31. Laidler KJ (1969) Theories of chemical reaction rates. McGraw-Hill, New York
32. Messer BM, Elrod MJ (1999) Chem Phys Lett 301:10–18
33. Espinosa-García J (1999) Chem Phys Lett 315:239–247
34. Notario R, Castaño O, Abboud JLM (1996) Chem Phys Lett 263:367–370
35. Jodkowski JT, Rayez MT, Rayez JC, Bérces T, Dóbé S (1998) J Phys Chem A 102:9219–9229
36. Jodkowski JT, Rayez MT, Rayez JC, Bérces T, Dóbé S (1998) J Phys Chem A 102:9230–9243
37. Jodkowski JT, Rayez MT, Rayez JC, Bérces T, Dóbé S (1999) J Phys Chem A 103:3750–3765
38. Burk P, Koppel IA, Rummel A, Trumlar A (2000) J Phys Chem A 104:1602–1607
39. Sander SP, Friedl RR, Ravishankara AR, Golden DM, Kolb CE, Kurylo MJ, Molina MJ, Moortgat GK, Keller-Rudek H, Finlayson-Pitts BJ, Wine PH, Huie E, Orkin VL (2006) Chemical kinetics and photochemical data for use in atmospheric studies, Evaluation Number 15, NASA Panel for Data Evaluation, NASA. Jet Propulsion Laboratory, California Institute of Technology, Pasadena, CA
40. Atkinson R, Baulch DL, Cox RA, Crowley JN, Hampson RF, Hynes RG, Jenkin ME, Rossi MJ, Troe J, IUPAC Subcommittee (2006) Evaluated kinetic and photochemical data for atmospheric chemistry: Volume II – gas phase reactions of organic species. Atmos Chem Phys 6:3625–4055
41. Garrett BC, Truhlar DG (1979) J Phys Chem 83:200–203
42. Troe J (1994) J Chem Soc Faraday Trans 90:2303–2317